

Supplemental Material

Gapless quantum spin liquid ground state in the two-dimensional spin-1/2 triangular antiferromagnet YbMgGaO_4

Yuesheng Li¹, Haijun Liao², Zhen Zhang³, Shiyan Li³, Feng Jin¹, Langsheng Ling⁴, Lei Zhang⁴, Youming Zou⁴, Li Pi⁴, Zhaorong Yang⁵, Junfeng Wang⁶, Zhonghua Wu⁷, and Qingming Zhang^{*,1,8}

¹Department of Physics, Renmin University of China, Beijing 100872, P. R. China

²Institute of Physics, Chinese Academy of Sciences, Beijing 100190, P. R. China

³State Key Laboratory of Surface Physics, Department of Physics, and Laboratory of Advanced Materials, Fudan University, Shanghai 200433, P. R. China

⁴High Magnetic Field Laboratory, Chinese Academy of Sciences, Hefei 230031, P. R. China

⁵Institute of Solid State Physics, Chinese Academy of Sciences, Hefei 230031, P. R. China

⁶Wuhan National High Magnetic Field Center, Wuhan 430074, P. R. China

⁷Institute of High Energy Physics, Chinese Academy of Science, Beijing 100049, P. R. China

⁸Department of Physics and Astronomy, Collaborative Innovation Center of Advanced Microstructures, Shanghai Jiao Tong University, Shanghai 200240, P. R. China

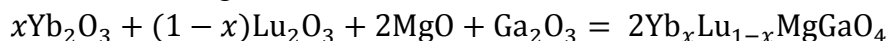
*e-mail: qmzhang@ruc.edu.cn

We present here:

1. Material synthesis and measurement details
2. Synchrotron X-ray diffractions and structure refinements of YbMgGaO_4 and LuMgGaO_4
3. Low-temperature XRD patterns of YbMgGaO_4 .
4. ESR spectra of YbMgGaO_4 and $\text{Yb}_{0.04}\text{Lu}_{0.96}\text{MgGaO}_4$ samples
5. Linear fit to the magnetization data of YbMgGaO_4 in the constant susceptibility range (from 1.6 to 2.8 T) at 0.5 K

1. Material synthesis and measurement details

$\text{Yb}_x\text{Lu}_{1-x}\text{MgGaO}_4$ ($x = 1, 0.4, 0.16, 0.08, 0.04$ and 0) powder samples were prepared via the following chemical reaction:



Stoichiometric mixtures of high-purity Yb_2O_3 (99.99%), Lu_2O_3 (99.9%), MgO (99.99%) and Ga_2O_3 (99.999%) were ground, pressed into tablets and heated in air at $1450\text{ }^\circ\text{C}$ for 4 days with an intermediate grinding step. Almost no sample mass loss was observed after heating.

To remove the influence of a possible preferred orientation of the powder samples during the crystal-structure refinements, the solid-phase, synthesized samples were carefully ground into powders with particle sizes smaller than $\sim 5\text{ }\mu\text{m}$, as determined by microscope observations. The powder samples were diluted with a moderate amount of glue, packed into capillaries ($D = 0.2\text{ mm}$) and prepared for X-ray diffraction using the MYTHEN detector at the diffraction station (4B9A) of the Beijing Synchrotron Radiation Facility.

For the magnetization and electron spin resonance (ESR) spectrum measurements, at least two independent powder samples were prepared and measured for each magnetic $\text{Yb}_x\text{Lu}_{1-x}\text{MgGaO}_4$ composition. In addition, no clear effects caused by the possible preferred orientation of the samples were observed from the measurements.

The ESR measurements were performed using a Bruker EMX plus 10/12 CW-spectrometer at X-band frequencies ($f \sim 9.4\text{ GHz}$); the spectrometer was equipped with a continuous He gas-flow cryostat.

The residuals in all fits and refinements are defined as

$$R_p = \frac{\sum |y_o - y_c|}{\sum |y_o|} \quad (1)$$

where, y_o and y_c are observed and calculated values respectively. International system of units (SI) was used.

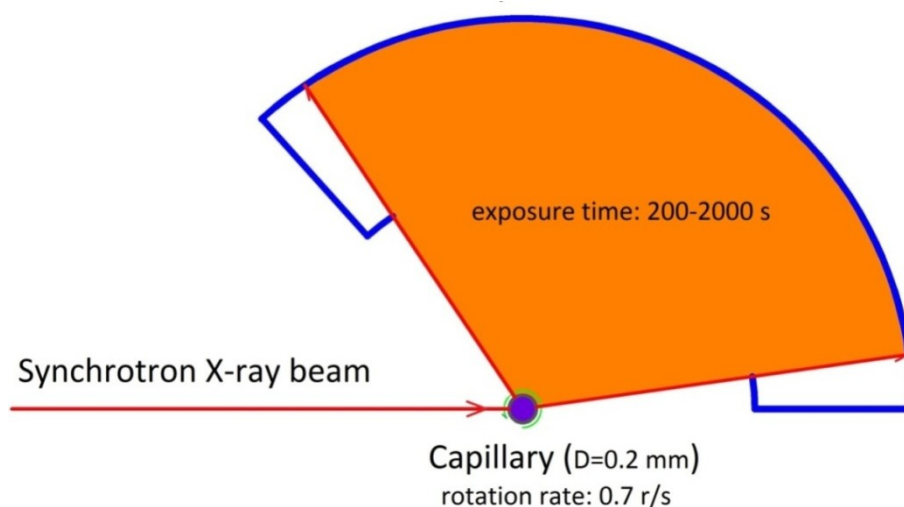


Figure S1. Diagram of the MYTHEN detector installed at the diffraction station (4B9A) of the Beijing Synchrotron Radiation Facility.

2. Synchrotron X-ray diffractions and structure refinements of YbMgGaO₄ and LuMgGaO₄

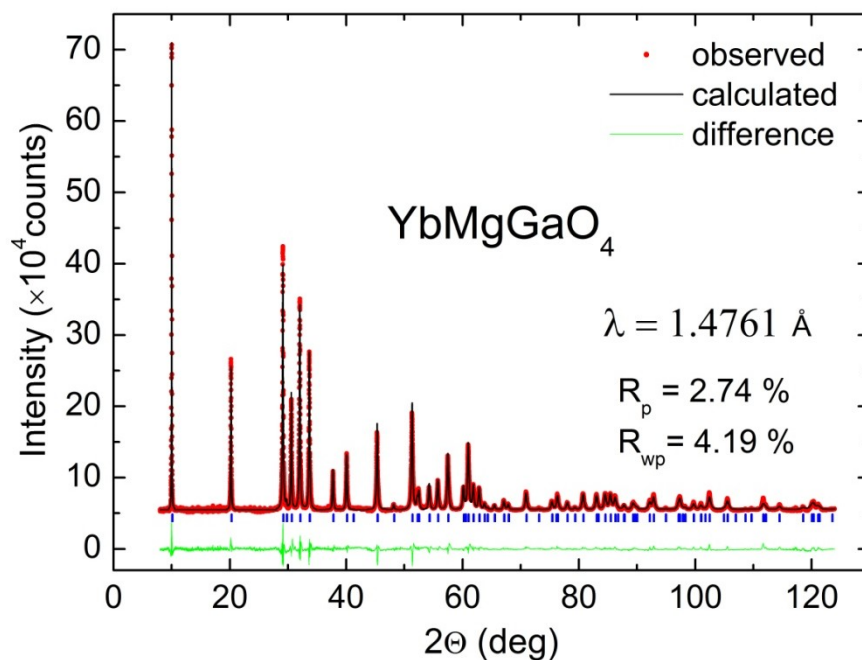


Figure S2. Synchrotron X-ray diffraction and final Rietveld refinement profiles for YbMgGaO₄ at 300 K.

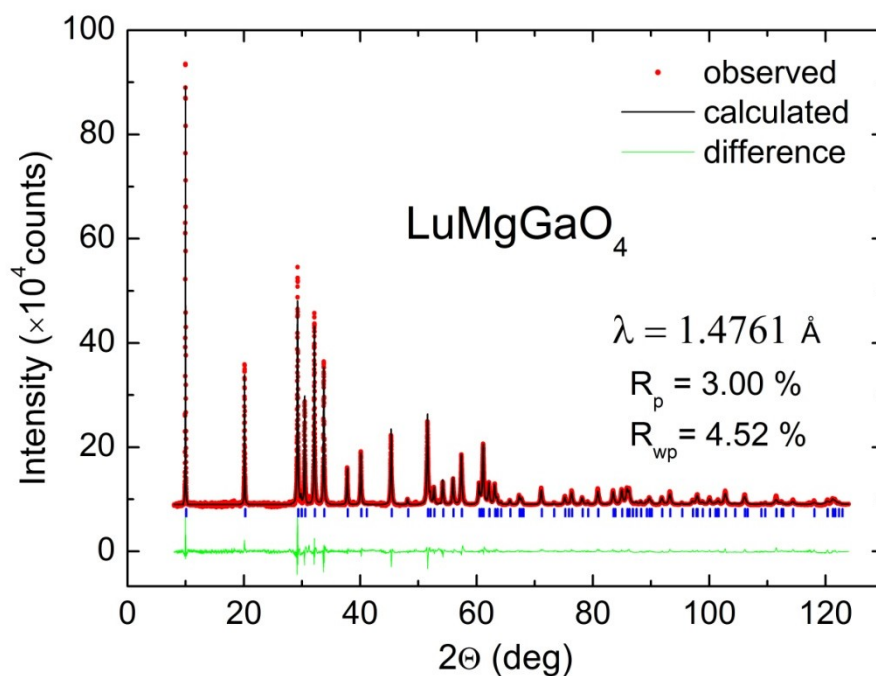


Figure S3. Synchrotron X-ray diffraction and final Rietveld refinement profiles for LuMgGaO₄ at 300 K.

Table S1. Refined crystal structures of YbMgGaO₄ and LuMgGaO₄

Compound		YbMgGaO ₄		LuMgGaO ₄	
Model		I	II	I	II
Space group		$R\bar{3}m$			
Lattice	a (Å)	3.40212(8)	3.40282(6)	3.38750(5)	3.38750(5)
	c (Å)	25.1191(6)	25.1243(5)	25.2069(4)	25.2071(4)
Yb/Lu ³⁺	Fraction	1	0.5	1	0.5
	z	0	0.00439(6)	0	0.00425(6)
	Uiso (×100)	1.016(18)	0.751(21)	0.981(18)	0.637(20)
Mg ²⁺ /Ga ³⁺	Fraction	0.5	0.5	0.5	0.5
	z	0.214902(29)	0.214918(29)	0.215397(30)	0.215385(30)
	Uiso (×100)	0.216(26)	0.301(26)	0.332(27)	0.226(27)
O1 ⁻²	z	0.29260(10)	0.29221(10)	0.29177(11)	0.29213(11)
	Uiso (×100)	0.92(8)	0.72(8)	1.15(8)	1.04(8)
O2 ⁻²	z	0.12967(9)	0.12993(9)	0.12967(10)	0.12971(10)
	Uiso (×100)	0.54(8)	0.47(7)	1.02(8)	0.68(7)
Residuals	R_{wp}	0.0419	0.0412	0.0452	0.0442
	R_p	0.0274	0.0268	0.0300	0.0292

3. Low-temperature XRD patterns of YbMgGaO₄.

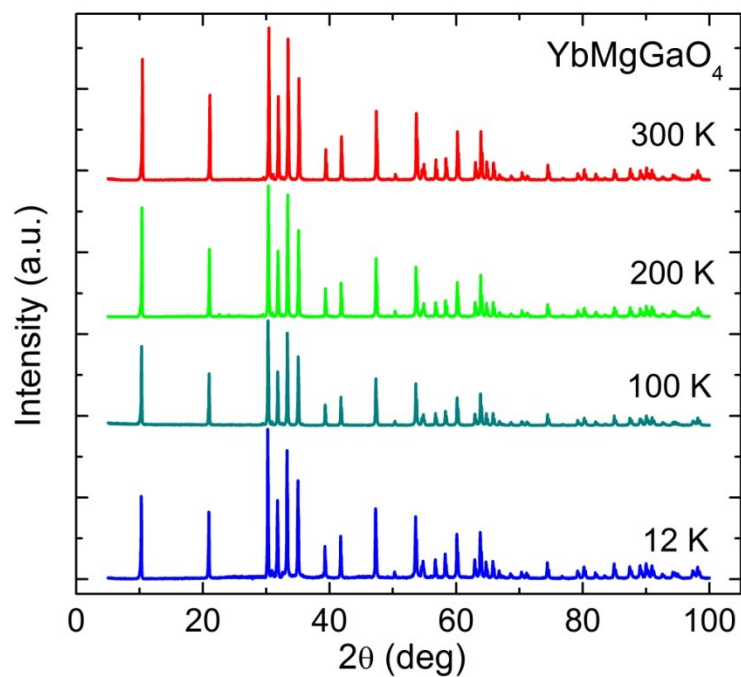


Figure S4. X-ray (Cu-K_α) diffraction profiles for YbMgGaO₄ at 300, 200, 100 and 12 K respectively. No additional reflections are observed at temperatures down to 12 K, indicating that no structural transitions occurred.

4. ESR spectra of YbMgGaO_4 and $\text{Yb}_{0.04}\text{Lu}_{0.96}\text{MgGaO}_4$ samples

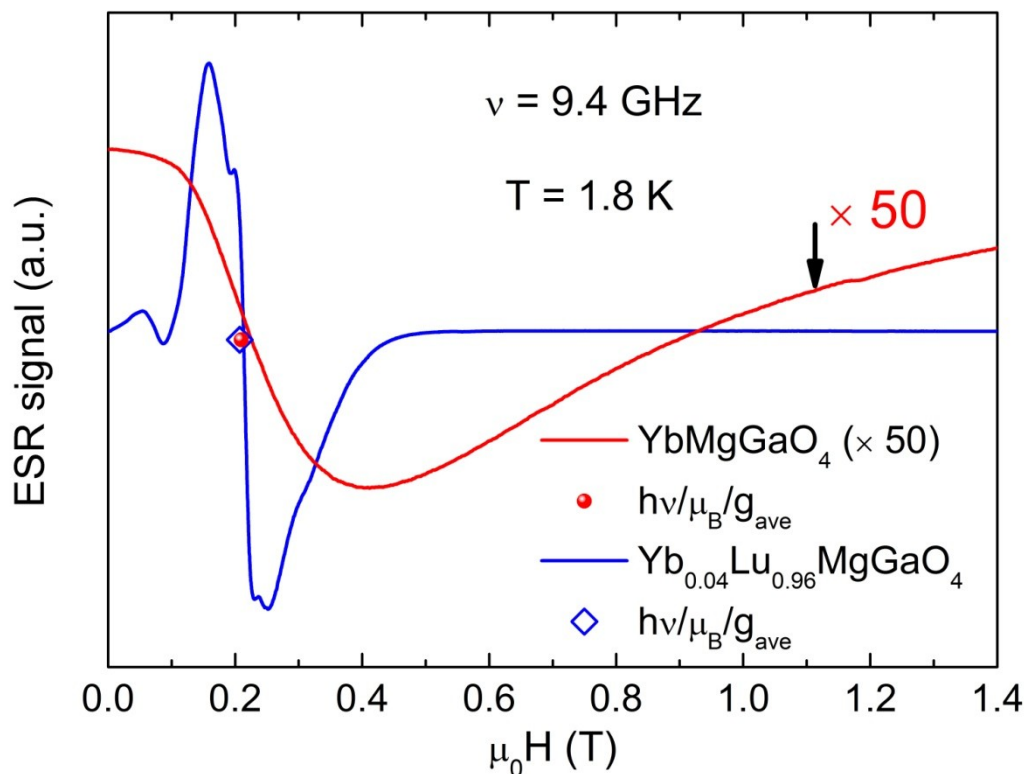


Figure S5. X-band (9.4 GHz) Yb^{3+} first-derivative absorption ESR spectra for YbMgGaO_4 and $\text{Yb}_{0.04}\text{Lu}_{0.96}\text{MgGaO}_4$. The narrow and intense hyperfine lines¹ observed in the quasi-free spin compound $\text{Yb}_{0.04}\text{Lu}_{0.96}\text{MgGaO}_4$ completely disappear in the spectrum of YbMgGaO_4 , suggesting that no observable isolated Yb^{3+} or magnetic defects ($< 0.04\%$) are present in YbMgGaO_4 .

5. Linear fit to the magnetization data of YbMgGaO₄ in the constant susceptibility range (form 1.6 to 2.8 T) at 0.5 K

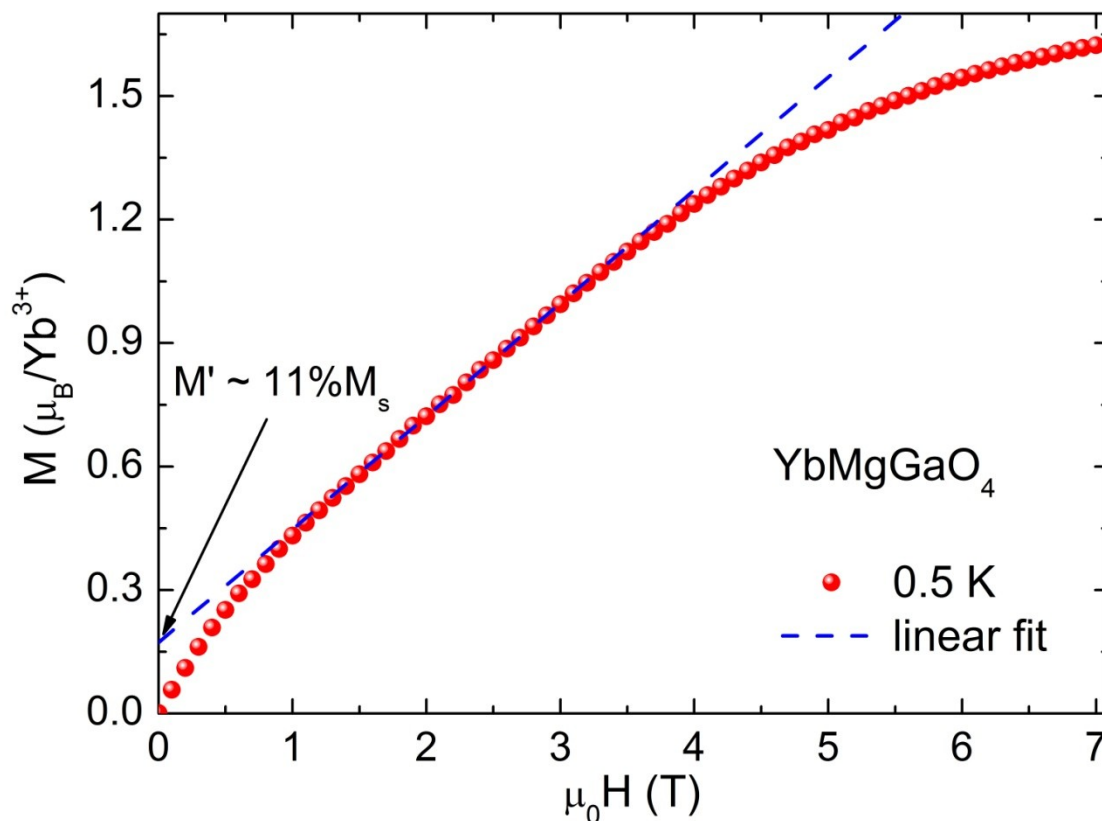


Figure S6. Linear fit to the magnetization data of YbMgGaO₄ in the constant susceptibility range (form 1.6 to 2.8 T) at 0.5 K. The fitted intercept, $\sim 0.173(4) \mu_B/Yb^{3+}$ (the convex magnetization), gives $\sim 11\%$ of the saturation magnetization.

References

1. Misra, S. K. & Isber, S. EPR of the Kramers ions Er³⁺, Nd³⁺, Yb³⁺ and Ce³⁺ in Y(NO₃)₃·6H₂O and Y₂(SO₄)₃·8H₂O single crystals: Study of hyperfine transitions. *Physica B* **253**, 111-122 (1998).